Viscoelastoplastic & thixotropic predictions for sharp-corner contraction-expansion circular flows with time-dependent constitutive equations

J. Esteban López-Aguilar[1], Michael F. Webster[1], Hamid R. Tamaddon-Jahromi[1], and Octavio Manero[2]

[1] Institute of Non-Newtonian Fluid Mechanics, Swansea University, College of Engineering, Bay Campus, Fabian Way, Swansea, SA1 8EN, UK
[2] Instituto de Investigaciones en Materiales, UNAM, 04510, Mexico.

ABSTRACT

A comparative analysis is performed for *time-dependent* and *viscoelastoplastic* fluids using revised BMP+_τ_p and De Souza models. In the *plastic-regime ($Q<<1;\beta\leq10^{-1}$):* yield-stress and strain-hardening promote solid-like features (augmented unyielded regions), whilst elasticity stimulates asymmetry. In the *viscoelastic—regime ($Q>1;\beta\geq10^{-1}$):* there is complex interplay between pure-extension (centreline) and pure-shear (walls/recirculation-zones; lip-vortices).

INTRODUCTION

Viscoelastoplastic fluids exhibit a so-called *'yield stress'*, that governs the transition from solid-like to liquid-like response, in combination with viscoelastic features. These fluids develop stagnation regions, where the material does not deform plastically due to elastic resistance from the microstructure. Hence, their velocity gradients vanish in these regions[1]. This study is concerned with viscoelastoplastic flow using thixotropic constitutive equations in complex flow. The rheology of *worm-like micellar* systems dynamically adjusts to conform to prevailing environmental conditions, hence the term *'smart materials'*[1,2]. These are amongst the many features that render such systems as ideal candidates for varied processing and industrial applications. Examples of typical industrial applications of relevance include - use as drilling fluids in enhanced oil-reservoir recovery (EOR), additives in house-hold-products, paints, slurries, pastes and some food products, pastes, some food products cosmetics, health-care products, and as drag reducing agents[1,2]. In this study, the *plastic regime* is studied at low flow-rates (Q) for extremely concentrated fluids (solvent fraction, $\beta<10^{-1}$). Here, elasticity-increase causes asymmetry about the contraction-plane, whilst yield-stress and enhanced strain-hardening promote solid-like features, apparent through augmented unyielded regions and rising pressure-drops. Concerning *viscoelastic response* (larger-Q; minimised plasticity; β=1/9), vortex-structure reflects a complex interplay between the pure-extensional centreline-flow and the pure-shear flow deformation along the walls and in recirculation-zones

GOVERNING EQUATIONS & THEORETICAL FRAMEWORK

In non-dimensional form, the mass and momentum equations may be expressed, under incompressible and isothermal conditions, as:

$$\nabla \cdot \boldsymbol{u} = 0\,, \tag{1}$$

$$Re\frac{\partial \boldsymbol{u}}{\partial t} = \nabla \cdot \boldsymbol{T} - Re\boldsymbol{u}\cdot\nabla\boldsymbol{u} - \nabla p\,. \tag{2}$$

Here, t represents time, spatial-gradient and divergence differential operators apply over the problem domain, with field variables $\boldsymbol{u}$, p and $\boldsymbol{T}$ of fluid-velocity, hydrodynamic-pressure and total viscoelastic-stress contributions, respectively. Then, the total viscoelastic-stress ($\boldsymbol{T}$) may be segregated into two parts: a solvent-component $\boldsymbol{\tau}_s$ (viscous-inelastic $\boldsymbol{\tau}_s = 2\beta\boldsymbol{D}$), and a polymeric nonlinear-component $\boldsymbol{\tau}_p$. Though plasticity may be introduced into either solvent or polymeric components, or indeed both, here the theme is to consider only contributions arising from those of a polymeric source. $\boldsymbol{D} = (\nabla\boldsymbol{u} + \nabla\boldsymbol{u}^{\mathrm{T}})/2$ is the rate-of-deformation tensor, for which superscript 'T' denotes tensor-transpose operation. A characteristic time $\left(\frac{L}{U}\right)$ is used to non-dimensionalise time t and $\boldsymbol{D}$, where U and L are taken as characteristic velocity and length, respectively; internal stress and hydrostatic pressure are normalised with a characteristic stress measured at the so-called first Newtonian plateau $\left(\eta_{p0} + \eta_s\right)\frac{U}{L}$. In addition, this provides for a reference viscosity zero shear-rate viscosity, $\eta_{p0} + \eta_s$, in the viscoelastic regime, with zero-rate polymeric-viscosity η_{p0}, and η_s the constant solvent-viscosity. Based upon these definitions, a solvent-fraction $\beta = \eta_s / \left(\eta_{p0} + \eta_s\right)$ may be adopted, extracting the non-dimensional group Reynolds number $Re = \rho UL / \left(\eta_{p0} + \eta_s\right)$, with material density, ρ. Elasticity is interpreted through the non-dimensional group Weissenberg number, $Wi = \lambda_1 U / L$, defined on the product of a characteristic material relaxation-time ($\lambda_1 = \frac{\eta_{p0}}{G_0}$), and a characteristic rate-scale (U/L; inverse of the characteristic time). Hence, a general space-time differential statement for the stress equation-of-state may be expressed as:

$$Wi\overset{\nabla}{\boldsymbol{\tau}}_p = 2\left(1-\beta\right)\boldsymbol{D} - f\boldsymbol{\tau}_p, \qquad (3)$$

where $\overset{\nabla}{\boldsymbol{\tau}}_p$ is the upper-convected derivative of extra-stress. In addition, the material structure is incorporated through the pre-functional f, which products the polymeric stress.

The BMP+_τ_p model

Considering derivation through the BMP-family of thixotropic constitutive models, the non-linear f-functional is related explicitly to the viscosity of the fluid, as a dimensionless fluidity[1,2]. In the present study, a novel and revised model-variant is proposed, via the *so-called* BMP+_τ_p model. This new BMP+_τ_p model enjoys such benefits as: the inclusion of a relaxation-time (elasticity) in the fluid-structure construction-destruction dynamics; whilst retaining a modified non-linear destruction-term. These BMP+_τ_p features provide simultaneously two key experimental-manifestations in wormlike micellar and concentrated polymer solution rheology: first, a bounded extensional-viscosity η_{Ext}-response; and secondly, a first normal-stress in shear (N_{1Shear}) with upturn at high deformation rates. Accordingly, the thixotropic BMP+_τ_p f-functional evolution obeys the partial differential equation:

$$\left(\frac{\partial}{\partial t} + \boldsymbol{u}\cdot\nabla\right)f = \frac{1}{\omega}\left(1-f\right) + \left(\xi_{G_0}Wi - \xi f\right)\left|\boldsymbol{\tau}_p : \boldsymbol{D}\right| \qquad (4)$$

Here, dimensionless micellar-structure coefficients appear in Eq. 4 within the corresponding dynamic structure-mechanism terms: structure-construction

($\omega = \lambda_s \frac{U}{L}$) and structure-destruction ($\xi_{G_0} = \frac{k_0 G_0}{\eta_\infty + \delta}\left(\eta_{p0} + \eta_s\right)$ and $\xi = k_0\left(\eta_{p0} + \eta_s\right)\frac{U}{L}$).

In this analysis, numerical computations are performed with a hybrid finite volume/element time-stepping algorithm, of multi-stages per time-step; whilst incorporating an incremental pressure-correction scheme. New and novel aspects to the computational procedures include - imposing velocity gradient boundary conditions at the flow centreline (*VGR*-correction); a discrete correction for exact continuity-satisfaction; absolute-representation for the constitutive-model structure function (*ABS-f*); and adopting solution continuation through steady-states whilst increasing flow-rate (and not fluid elasticity), see for example López-Aguilar et al.[1,2].

The De Souza model

In the current study, the De Souza stress equation is re-cast into a split form $\boldsymbol{T} = \boldsymbol{\tau}_s + \boldsymbol{\tau}_p$ (originally presented in total-stress form; de Souza[3], de Souza and Thompson[4]), with the solvent-contribution $\boldsymbol{\tau}_s$ of constant viscosity Newtonian-type. Then evolution of the non-dimensional polymeric-stress component may represented as:

$$Wi\overset{\nabla}{\boldsymbol{\tau}}_p = 2\frac{(1-\beta)}{\lambda^m}\boldsymbol{D} - f\boldsymbol{\tau}_p, \qquad (5)$$

where the *f*-functional is defined as $f = \frac{1}{\lambda^m}\left(\eta_{p0}/\eta_p\right)$, the polymeric viscosity is $\eta_p(\lambda) = \left(\frac{\eta_{p0}}{\eta_s}\right)^{\lambda} - 1$, and the structural modulus is $\frac{G_s(\lambda)}{G_0} = \frac{1}{\lambda^m}$. Note that the structure parameter λ appears as an inverse factor in the dissipation-term in Eq. 5, but also within the *f*-functional and the shear-modulus definitions. This suggests a more complex De Souza-type fluid-structure/material-property dependency.

Accordingly, the De Souza structure-parameter evolution equation for λ is:

$$\left(\frac{\partial}{\partial t} + \boldsymbol{u}\cdot\nabla\right)\lambda = \frac{1}{\omega_{DS}}\left[(1-\lambda)^a + (1-\lambda_{ss})^a\left(\frac{\lambda}{\lambda_{ss}}\right)^b\right] \qquad (6)$$

where, $\omega_{DS}=t_{eq}U/L$ is a dimensionless parameter for λ. As such, Eq. 6 states a new and *corrected form* of De Souza structure-equation. This now follows the developments outlined by de Souza and Thompson[4], and López-Aguilar et al.[1], wherein any inconsistency in response noted in dimensionless stress, arising from the destruction term, has been accounted for. The exponents *a*, *b* and *m* are dimensionless positive constants (taken as unity in the present study). Then, the associated steady-state structure parameter λ_{ss} is defined as:

$$\lambda_{ss}\left(II_D\right) = \frac{ln\,\eta_{ss}\left(II_D\right) - ln\,\eta_s}{ln\,\eta_{p0} - ln\,\eta_s}, \qquad (7)$$

and the steady-state viscosity η_{ss} is:

$$\eta_{ss}\left(II_D\right) = \left[1 - exp\left(-\frac{II_D}{\tau_0}\right)\right]\times \left[\frac{\tau_0 - \tau_{0d}}{II_D}exp\left(-\frac{II_D}{\dot{\gamma}_{0d}}\right) + \frac{\tau_{0d}}{II_D} + KII_D^{\,n-1}\right] + \beta \qquad (8)$$

In Eq. 8, the dynamic and static yield-stress parameters are τ_0 and τ_{0d}, respectively; $\dot{\gamma}_{0d}$ is the shear-rate that denotes the transition between τ_0 to τ_{0d}. Then, *K* and *n* are

consistency and power-law indexes, respectively.

RESULTS

Plastic regime

Low flow-rates (Q≤10) and extremely high polymer concentrations (β≤10^{-1}); Moderate Hardening fluids

Fig. 1 illustrates *De Souza* solutions, upon selecting the highly-polymeric concentration (β=1/9) to establish a common comparison-basis with BMP+_τ_p predictions. The criterion to discern the yielded fluid from unyielded solid-like material is derived through the second invariants of polymeric-stress, $II_{\boldsymbol{\tau}_p} = \sqrt{\frac{1}{2} tr\boldsymbol{\tau}_p^2}$. Then, at fixed Q=1 and under yield-stress parameters τ_0=τ_{0d}=0.02, an X-shaped yield-front region is identified. This asymmetrical pattern about the contraction-plane, is retrieved from imbalanced unyielded-zones in the recess-corners. Subsequent and rising yield-stress influence (τ_{0d}≥0.05), renders shrinking *double-claw* unyielded regions, which are confined to the contraction-gap neighbourhood. Conversely, with Q-rise, a sequence of fixed-τ_{0d}=0.1 solutions, commence from a symmetrical *eight-petal* and yielded-structure, which is confined to the constriction-zone. Then, at an intermediate Q-range (0.5≤Q≤1), the eight-petal structure gives way to a *four-petal/shamrock-shaped* unyielded-zone. Finally, at relatively high-Q (Q≥5), the ever-expanding yield-fronts of the contraction-flow zone, link-up with those from the upstream- and downstream-wall flow regions. Here, elastic-effects become prominent, with larger asymmetrical upstream yielded-zones appearing in the corner-recess regions. Comparatively, *across models* and at low flow-rates, *BMP+_τ_p solutions* (Fig. 2) reveal similar yield-front response to De Souza-solutions. In contrast however, at high flow-rates (Q>5), not shown) and extremely low solvent-fractions (β≤0.005), ever expanding yielded-regions are recorded that are slightly more prominent under De Souza representation, with marked asymmetrical unyielded-zones in the recess corners. One comments that, under *BMP+_τ_p* and with rise in polymeric-concentration - *at low flow-rates*, plastic features are promoted (see Q<5 solutions); whilst, at *sufficiently large flow-rates*, pronounced shear-thinning is provoked, resulting in enhanced fluid-response type regions (see Q=5 fields).

Viscoelastic regime

Polymer-concentration (1-β)-variation; Strong Hardening fluids - BMP+_τ_p

A range of solvent-fractions of β={1/9, 0.5, 0.7, 0.8, 0.9} are studied (vortex-intensity Ψ_{min} Fig. 3 {β=0.5 and β=0.8 results not shown}, streamlines Fig. 4), under strong-hardening SH-conditions, principally with focus upon vortex-phasing (*lip-vortex formation)*. Under polymer-concentration (1-β)-increase, Ψ_{min} is reflected in Fig. 3. In general and *upstream* of the contraction, solute-content (1-β)-increase elevates segregating response. With Q-rise, Ψ_{min} appears flatter in solvent-dominated fluids (β=0.9), whilst it sharply rises for highly-polymeric fluids (β=1/9). This is accompanied by a *change in vortex-cell shape and traversal of rotation-loci*. As described under hardening-changes above, diminished *downstream*-activity appears to balance that in the upstream of the contraction; only adjusting with (1-β) change. *With (1-β)-increase, yet still within the dilute-regime (β={0.8, 0.7})*, Ψ_{min} is seen to somewhat enhance with Q-increase; in the largest-Ψ_{min} recorded (β=0.7, Q=10), Ψ_{min} is some 4.5-times stronger than that

observed in the solvent-dominated β=0.9-case (Fig. 3). Conspicuously, in terms of vortex-structure (of Fig. 4), from initial symmetrical streamline patterns ($0.1 \leq Q \leq 1$; somewhat distorted with increase in polymer-concentration), *intermediate phases* of *sc*/lip-vortex (*lv*) *coexistence* are recorded ($1 \leq Q \leq 4$). Notably, *within the high-Q range* of $Q \geq 5$, each β={0.8, 0.7} solution-set has an alternative and different response to Q-rise. Under β=0.8, the coexistent sc-*lv* structures coalesce, and a single *sc*-vortex is recovered. In contrast, at slightly increased polymer-concentration (β=0.7), the *lv dominates* and becomes an *elastic-corner (ec) vortex*. Finally under *highly-polymeric fluids* ($\beta \leq 0.5$), a steep Ψ_{min}-rise is recorded with incrementation in flow-rate (Fig. 3). Such strong $\beta \leq 0.5$-Ψ_{min} behaviour is reflected in a *direct transition from sc- to ec-vortex* formation (Fig. 4).

CONCLUSIONS

This study has facilitated comparative prediction for two new versions of thixotropic and viscoelastoplastic models (BMP+_τ_p and De Souza), under circular sharp-cornered contraction-expansion flow with aspect-ratio α=10. Two main flow-regimes have been examined in detail under a flow-rate Q-incrementation procedure: firstly, under *viscoelastic-response*, in the high-Weissenberg setting; and secondly, under *plastic-response*, where predictions are explored for extremely concentrated fluids.

For strongly-hardening (SH) *BMP+_τ_p* fluids and considering *solute-concentration increase*, predictions for various solvent-fractions ($0.9 \leq \beta \leq 1/9$) reveal a complex evolution history, from salient-corner vortex activity for β=0.9, to strong elastic-corner vortices for β=1/9. Notably, intermediate β={0.7, 0.8} solutions display coexistence of both upstream lip- and salient-corner vortices; with greater polymer-concentration, lip-vortices tend to dominate and generate elastic-corner vortices. Under the *plastic regime*, in extremely concentrated conditions ($\beta \leq 1/9$) and low-to-moderate flow-rates ($0.1 \leq Q(Wi) \leq 10$) with Q-rise, BMP+_τ_p and De Souza yield-fronts reveal growing yielded-zones about the contraction-zone. These yielded-zones connect those arising in the constriction-region to those around the upstream and downstream-walls; gradually becoming asymmetrical with elevation in elasticity.

REFERENCES

1. López-Aguilar, J.E., Webster, M.F., Tamaddon-Jahromi, H.R., and Manero O. (2016) "A comparative numerical study of time-dependent structured fluids in complex flows", *Rheol. Acta,* **55** 197–214.

2. López-Aguilar, J.E., Webster, M.F., Tamaddon-Jahromi, H.R., and Manero O. (2016) "Convoluted models & high-Weissenberg predictions for micellar thixotropic fluids in contraction-expansion flows", *J. Non-Newtonian Fluid Mech.,* **232** 55–66.

3. De Souza, P.R. (2011) "Thixotropic elasto-viscoplastic model for structured fluids", *Soft Matter* **7** 2471-2483.

4. De Souza P.R. and Thompson R.L (2013) "A unified approach to model elasto-viscoplastic thixotropic yield-stress materials and apparent yield-stress fluids", *Rheol. Acta* **52** 673-694.

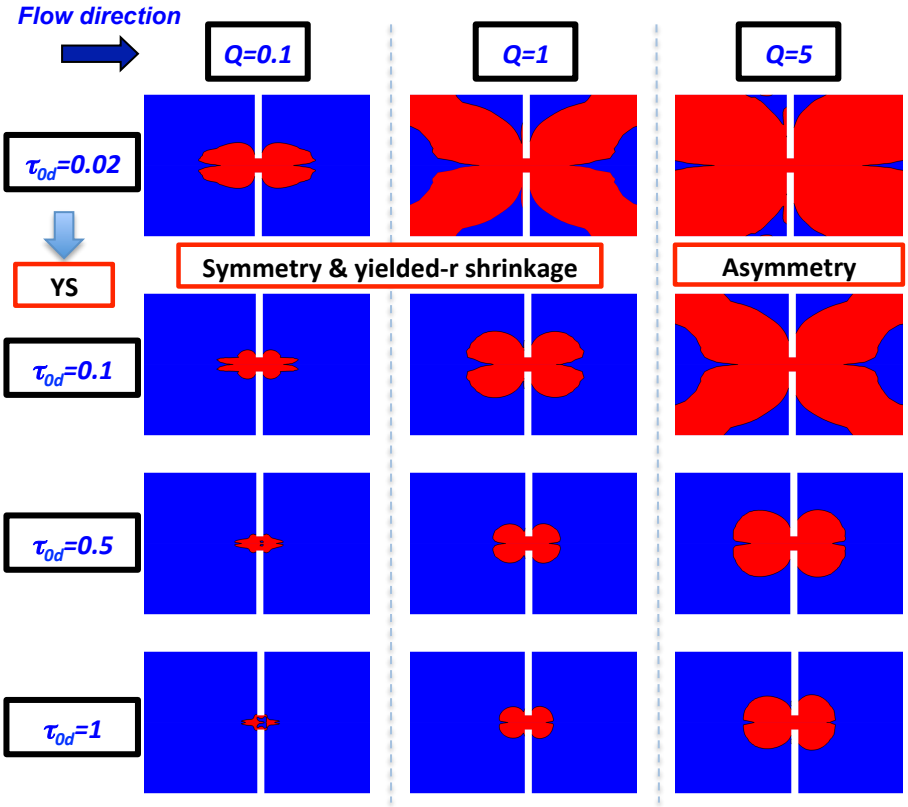

Figure 1. Yield-fronts; De Souza MH fluids; β=1/9; τ_{0d}={0.02, 0.1, 0.5, 1}

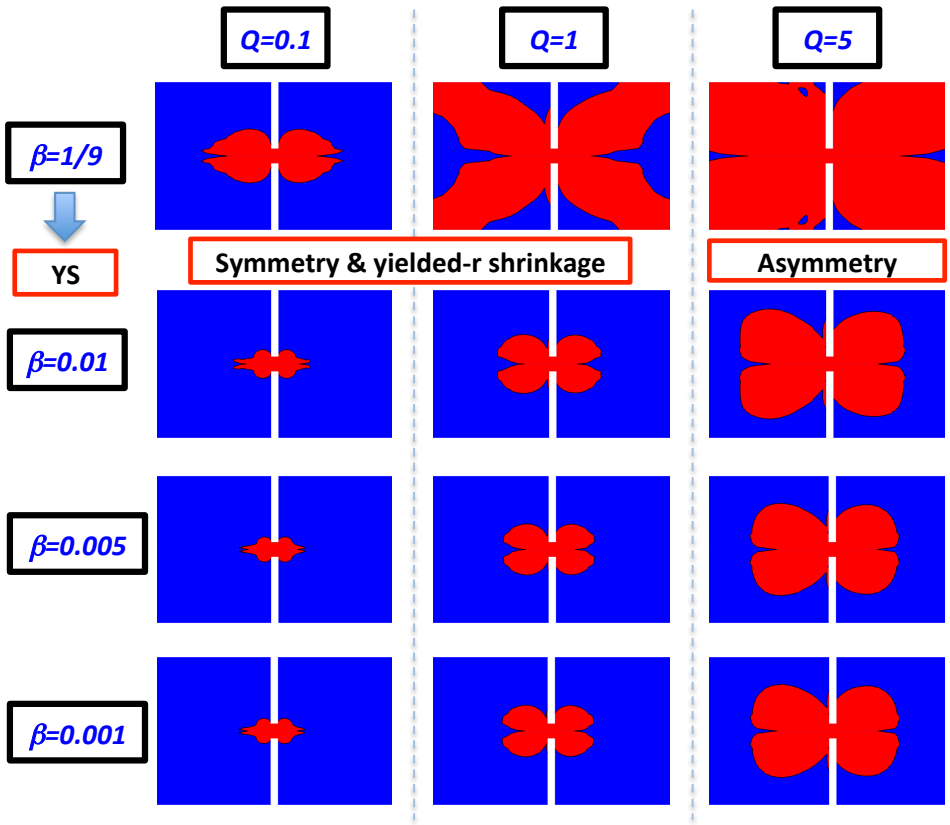

Figure 2. Yield-fronts; BMP+_τ_p MH fluids; β={1/9, 0.01, 0.005, 0.001}

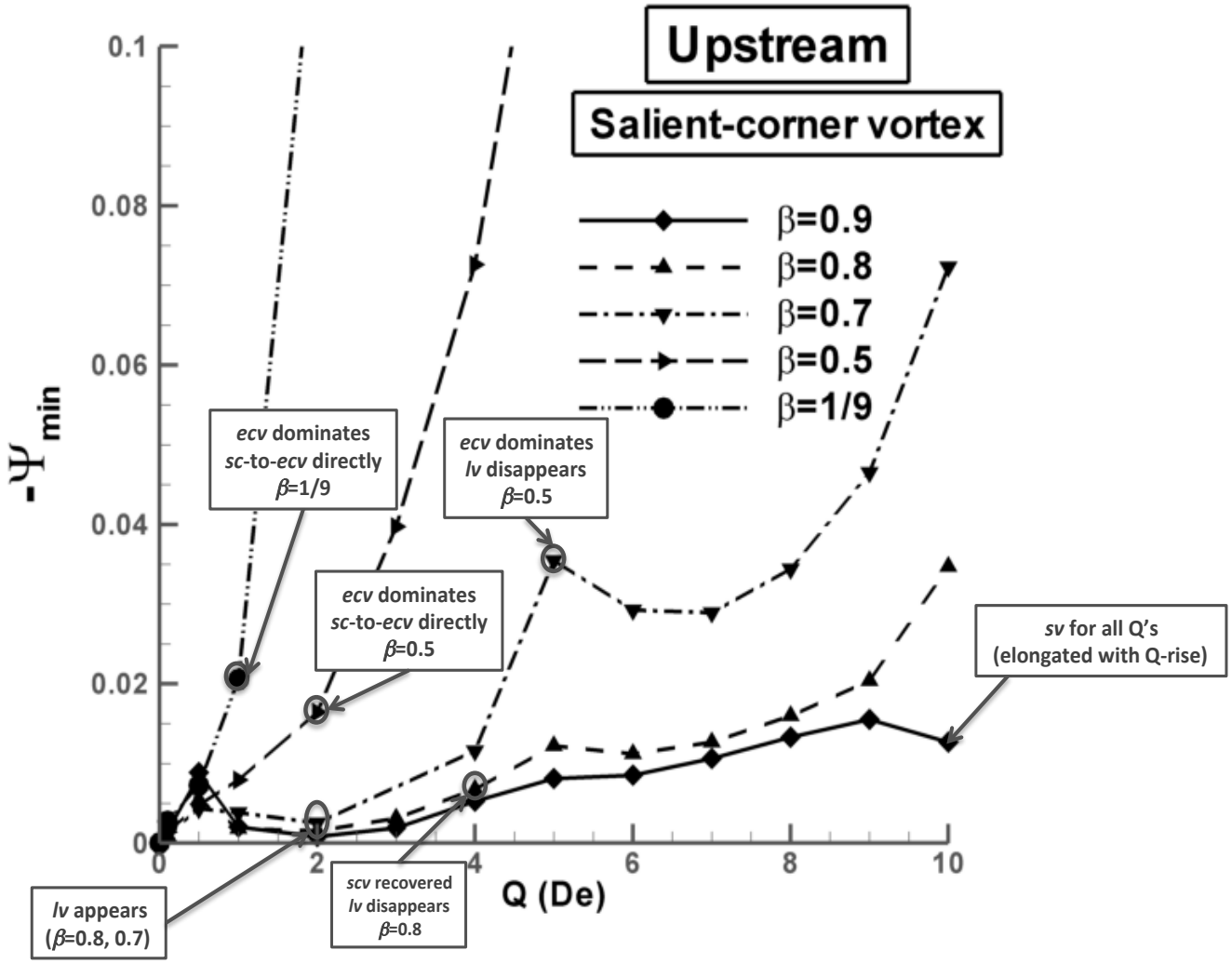

Figure 3. Vortex intensity; BMP+_τ_p SH fluids; β={0.9, 0.8, 0.7, 0.5, 1/9}

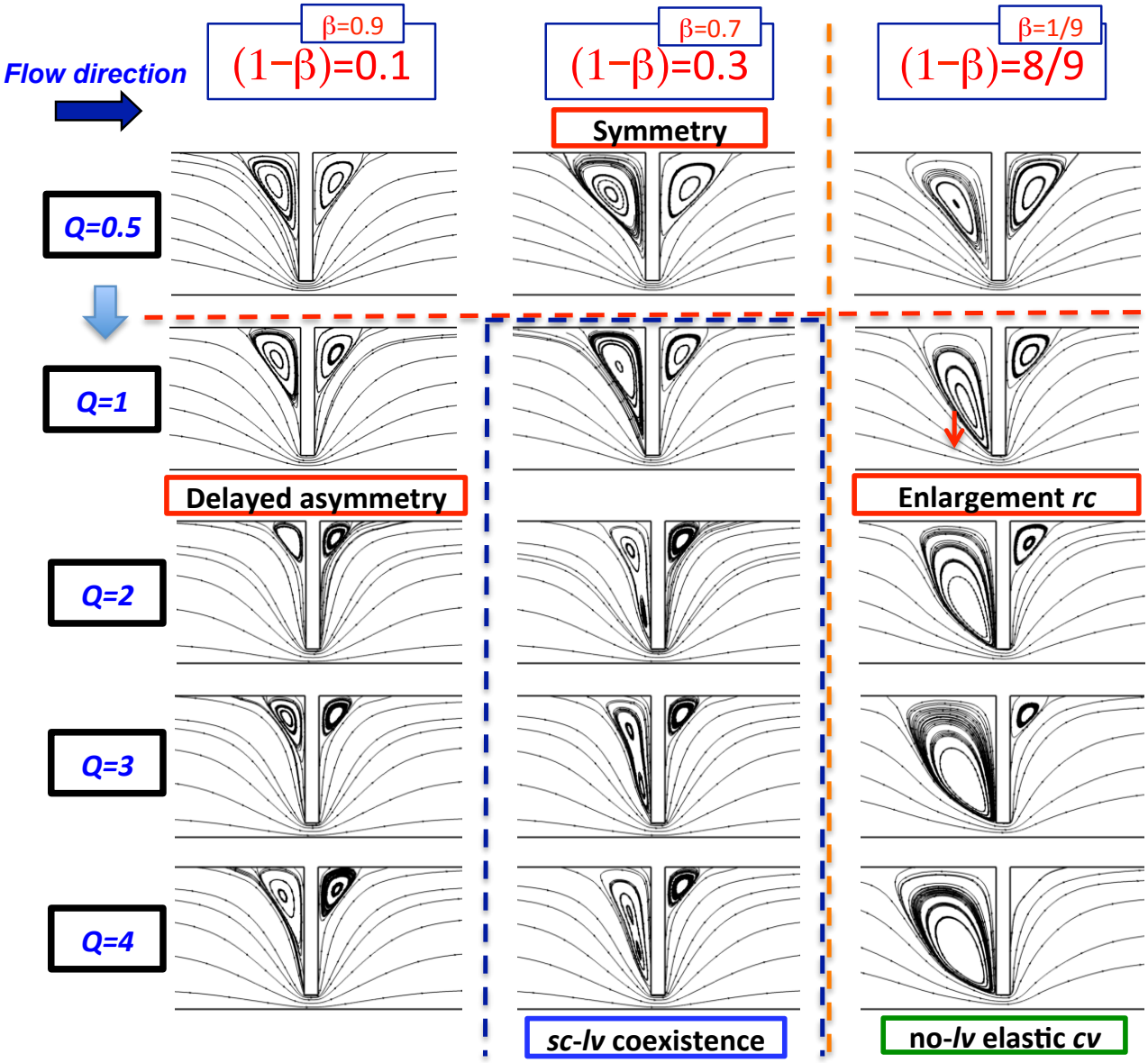

Figure 4. Streamlines; BMP+_τ_p SH fluids; β={0.9, 0.7, 1/9}